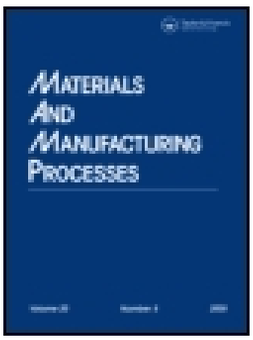

Materials and Manufacturing Processes

ISSN: 1042-6914 (Print) 1532-2475 (Online) Journal homepage: http://www.tandfonline.com/loi/lmmp20

Parametric optimization of abrasive water-jet machining processes using grey wolf optimizer

Shankar Chakraborty & Ankan Mitra

To cite this article: Shankar Chakraborty & Ankan Mitra (2018): Parametric optimization of abrasive water-jet machining processes using grey wolf optimizer, Materials and Manufacturing Processes

To link to this article: https://doi.org/10.1080/10426914.2018.1453158

Published online: 30 Mar 2018.

MATERIALS AND MANUFACTURING PROCESSES
https://doi.org/10.1080/10426914.2018.1453158

Taylor & Francis
Taylor & Francis Group

Parametric optimization of abrasive water-jet machining processes using grey wolf optimizer

Shankar Chakraborty and Ankan Mitra

Department of Production Engineering, Jadavpur University, Kolkata, India

ABSTRACT

Abrasive water-jet machining (AWJM) is a hybrid advanced machining process, which can be economically applied to machine almost any kind of material. It employs a high velocity waterjet to propel abrasive particles through a nozzle on the workpiece surface for material removal. The machining performance of AWJM process naturally depends on its several control (input) parameters, like water pressure, nozzle diameter, jet velocity, abrasive concentration, nozzle tip distance etc., which have also predominant effects on its responses, i.e., material removal rate, surface roughness, overcut, taper etc. In this paper, a new evolutionary algorithm, i.e., grey wolf optimizer (GWO), a technique based on the hunting behavior of grey wolves, is applied for finding out the optimal parametric combinations of AWJM processes. The main advantage of this algorithm is that it does not accumulate towards some local optima, and the presence of a social hierarchy helps it in storing the best possible solutions obtained so far. The derived results using GWO exhibit a significant improvement in the response values as compared to the previous attempts for parametric optimization of AWJM processes while applying other algorithms.

ARTICLE HISTORY
Received 25 November 2017
Accepted 23 February 2018

KEYWORDS
Abrasive water-jet machining process; grey wolf optimizer; optimization; parameter; response

Introduction

In order to meet the present day industrial requirements of high quality and precise products having extremely complicated features, conventional material removal processes are being continuously replaced by the non-traditional machining (NTM) processes. These NTM processes can not only eliminate the complexity of the conventional machining processes but also provide better surface quality and high dimensional accuracy while generating intricate and complex shapes on different difficult-to-machine materials. Based on the material removal mechanism, the NTM processes can be categorized into electro-thermal processes (laser beam machining, electron beam machining, electro-discharge machining, etc.), electrochemical processes (electrochemical machining, electrochemical grinding, electro jet drilling, etc.), mechanical processes (abrasive jet machining (AJM), water-jet machining, ultrasonic machining, abrasive water-jet machining (AWJM), etc.), and chemical processes (chemical milling, photochemical milling, etc.).

Abrasive water-jet machining is one such NTM process which employs a mixture of water and abrasive particles in form of a high-velocity jet as a tool for removal of material from the workpiece surface. Water jet at high velocity propels abrasives in the mixing chamber and the mixture is then passed through a nozzle, which increases the velocity of the jet as well as guides it at a narrow zone for striking the workpiece surface. Thus, the abrasive water jet strikes on the workpiece at very high velocity and the material is removed by the erosive action of the abrasives. Brittle fracture takes place due to the hammering action of the abrasives on the workpiece and subsequently, the wear particles produced are removed from the machining zone by the water jet. One of the major advantages of AWJM process over AJM process is that no dust is produced since a mixture of water and abrasives is utilized for material removal. In this process, very high cutting speed can be achieved as compared to WJM process, because of the carrying medium, i.e., water. It generally helps in accelerating the abrasive particles to a higher speed, which can also be varied by changing water pressure and nozzle diameter accordingly. It is practically suitable to machine both harder as well as softer work materials, and as opposed to other NTM processes, there is no generation of thermal stress. However, residual stresses due to striking of high velocity abrasive particles are present locally, which decrease away from the kerf. It can too machine electrically non-conductive and hard-to-machine materials, specially sandwich-honeycomb structural materials for use in aerospace industries.

The performance of an AWJM process depends on its various machining parameters, like the diameter of the abrasive water-jet nozzle, feed rate of the nozzle, abrasive concentration, nozzle pressure, stand-off distance, abrasive grain size, etc. Each of these machining parameters has also an effect on the responses, i.e., material removal rate (MRR) and surface roughness (SR) of the AWJM process. It has been investigated that an increase in stand-off distance would cause a rapid decrease in the machined depth. Hashish[1] developed a mathematical model to predict the depth of machining based

CONTACT Shankar Chakraborty s_chakraborty00@yahoo.co.in Department of Production Engineering, Jadavpur University, S.C. Mullick Road, Kolkata 700032, India.
Color versions of one or more of the figures in the article can be found online at www.tandfonline.com/lmmp.

on a given set of AWJM process parameters. However, in order to achieve maximum MRR or minimum SR, a perfect parametric mix of various AWJM process parameters needs to be searched out. Several mathematical and analytical tools, like response surface methodology (RSM), artificial neural network (ANN), grey relational analysis (GRA), Taguchi robust design methodology etc. have already been deployed so as to model the interrelationships between AWJM process parameters and its responses, while providing the optimal combinations of different process parameters in order to satisfy various end-product requirements. Complexity in machining dynamics and material removal mechanism has forced the earlier researchers to find out optimal or near optimal machining conditions within discrete and continuous parametric spaces having multi-modal, differentiable or non-differentiable objective functions, formulated from the developed mathematical models. In this paper, grey wolf optimizer (GWO) which mimics the pack hunting behavior of grey wolves is applied for parametric optimization of two AWJM processes, and its performance is also validated with respect to other popular algorithms.

Jain et al.[2] considered two mathematical models for optimization of process parameters in AJM of brittle and ductile materials at normal impact of abrasive particles using genetic algorithm (GA), and investigated the causes of variation in MRR with respect to various decision variables (i.e., mass flow rate, mean radius and velocity of the abrasive particles). Çaydaş et al.[3] considered abrasive grit size, traverse speed, water-jet pressure, stand-off distance and abrasive flow rate as the most important parameters in an AWJM process, and predicted the SR value while employing ANN technique. Zain et al.[4] integrated simulated annealing (SA) and GA to determine the optimal AWJM process parameters leading to a minimum value of SR. While combining ANN and SA techniques, Zain et al.[5] estimated the optimal settings of traverse speed, water-jet pressure, stand-off distance, abrasive grit size and abrasive flow rate for achieving a minimum SR value. Aultrin et al.[6] presented a fuzzy logic-based modeling of AWJM process, and predicted the values of MRR and SR for different combinations of process parameters, like water-jet pressure at the nozzle exit, diameter of the abrasive water-jet nozzle, feed rate of the nozzle, mass flow rate of water and mass flow rate of the abrasives. Pawar and Rao[7] employed teaching-learning-based optimization (TLBO) algorithm for parametric optimization of an AWJM process and compared its performance with the other state-of-the-art optimization algorithms. Yusup et al.[8] applied artificial bee colony (ABC) algorithm to optimize the settings of five AWJM process parameters, i.e., traverse speed, water-jet pressure, stand-off distance, abrasive grit size and abrasive flow rate for achieving minimum SR value. It was also concluded that the optimization performance of ABC algorithm was superior to ANN, GA, and SA techniques. Mohamad et al.[9] employed cuckoo algorithm for prediction of SR value in AWJM process and concluded that it could outperform the optimization results of two well-known computational techniques, i.e., ANN and support vector machine. Aultrin and Anand[10] applied GRA technique for parametric optimization of five process parameters for AWJM of Aluminium 6061 alloy. Jagadish et al.[11] determined the optimal combinations of pressure within the pumping system, stand-off distance and nozzle speed in an AWJM process, while considering two process responses, i.e., SR and process time. Kubade et al.[12] studied the effects of water pressure, traverse speed, abrasive flow rate and stand-off distance of an AWJM process on MRR and SR. Lohar and Kubade[13] investigated the effects of different AWJM parameters (water pressure, feed rate, abrasive flow rate and stand-off distance) on MRR and SR while machining of high carbon high chromium steel (AISI D3). Shukla and Singh[14] applied firefly algorithm for determining the optimal values of the responses while considering the given ranges of the process parameters as the constraints. Dhanawade and Kumar[15] considered four important parameters (hydraulic pressure, traverse rate, stand-off distance, and abrasive mass flow rate) of an AWJM process and investigated their influences on delamination, kerf taper ratio and kerf top width. Nair and Kumanan[16] considered water pressure, abrasive flow volume, stand-off distance and table feed as the significant process parameters in AWJM of Inconel 617, and applied weighted principal component analysis (WPCA) method for optimizing six responses, i.e., MRR, circularity error, cylindricity error, axis perpendicularity error, surface perpendicularity error, and parallelism error. In all the previous attempts to optimization of multiple responses, weights assigned to different responses were assumed prior to optimization. However, no relevant guidance was provided regarding how to select those weights. In this paper, using GWO algorithm, a non-dominated set of Pareto solutions is provided for multi-response optimization, which guides the process engineers to select appropriate weights, as well as, being non-dominated, each solution is as good as the others in the Pareto set.

Materials and Methods

Grey wolf (*Canis lupus*), also known as a western wolf, is a canine native to the remote areas of Eurasia and North America, and is considered as one of the zenith predators, i.e., they are at the top of the food chain. The grey wolf is a social animal, whose basic social unit is a mated pair, i.e., a male and a female, and their offspring. On an average, a pack of grey wolves has a size of 5–11. They have a very strict social dominant hierarchy.

Their pack is divided into four groups, i.e., alpha, beta, delta, and omega, as shown in the hierarchical pyramid of Fig. 1. A male and a female are the leaders of the pack, called the alphas. All major decisions of hunting, sleeping place, time to wake up and so on, are taken by them. Their decisions are imposed on the whole pack. They are also called the dominant wolves in their pack and their orders should be followed by the pack. The second level of hierarchy in grey wolves is constituted by the beta. They are second in command to the alpha wolves and assist them in decision making and other activities of the pack. They can be either a male or female and is considered to be the leading candidate for the alpha position if an existing alpha passes away or becomes senile. They act as the advisors to the alpha and decision reinforcer to the rest of the pack. The lowest level of the hierarchy is

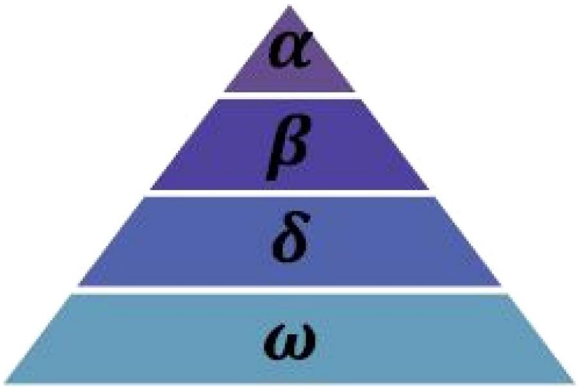

Figure 1. Social hierarchy of grey wolves.[17]

the omega. They have to report to the other dominant wolves and they are allowed to eat at the last in a pack. If a wolf is not an alpha, beta, or omega, it is a delta (sub-ordinate). They report to the alphas and betas, but are dominant over the omegas. Scouts, elders, hunters, sentinels, and caretakers belong to this category.[17]

Apart from the social hierarchy, grey wolves are also infamous about their group hunting pattern. According to Muro et al.,[18] the main phases of their hunting activity are shown in Fig. 2 and can be enumerated as below:

a. tracking, chasing and approaching the prey,
b. pursuing, encircling and harassing the prey until it stops moving, and
c. attack towards the prey.

In order to design and implement GWO algorithm, the above-mentioned hunting behavior and social hierarchy of grey wolves are mathematically modeled, as described in subsequent sub-sections.

The social hierarchy, tracking, encircling, and attacking the prey are discussed in the subsequent sections.[17]

Social hierarchy

In this model, the alpha (α) is considered to be the best solution, and beta (β) and delta (δ) are the second and third best solutions respectively. The rest of the population is assumed to be omega (ω). The hunting process is guided by the alpha, beta, and delta, and the omegas follow them.

Figure 2. Hunting pattern of grey wolves.[17]

Encircling the prey

Grey wolves have a distinct hunting pattern, i.e., they encircle their prey during the hunt. The following equations mathematically depict their encircling behavior.

$$\vec{D} = \left|\vec{C} \cdot \vec{X}_{\mathrm{p}}(t) - \vec{X}(t)\right| \tag{1}$$

$$\vec{X}(t+1) = \vec{X}_{\mathrm{p}}(t) - \vec{A} \cdot \vec{D} \tag{2}$$

where t indicates the most recent iteration, $\vec{A}$ and $\vec{C}$ are the coefficient vectors. The position vector of the prey is denoted by $\vec{X}_{\mathrm{p}}$ and the current position of the grey wolf is represented by $\vec{X}$. The vectors $\vec{A}$ and $\vec{C}$ can be calculated using the following two equations:

$$\vec{A} = 2\vec{a} \cdot \vec{r}_1 - \vec{a} \tag{3}$$

$$\vec{C} = 2 \cdot \vec{r}_2 \tag{4}$$

where components of $\vec{a}$ are linearly decreased from 2 to 0 over the entire course of iteration, and r_1 and r_2 are the random vectors in the interval [0,1]. The effects of these equations are illustrated in Figs. 3 and 4 respectively. The grey wolves can update their positions anywhere randomly, inside the space surrounding the prey, using Eqs. (1) and (2).

Hunting

Grey wolves are specialized in locating their prey and encircle it for hunting. The alpha wolf leads the hunt, the beta and delta follow the hunt occasionally. However, in a virtual search space, the location of the optimum (prey) is not known, so it is assumed that the alpha, beta, and delta have better knowledge about the location of the prey. Hence, the best solutions derived so far are stored in alpha, beta, and delta, and the omegas are obliged to update their positions with respect to the positions of alpha, beta, and delta, according to the following equations:

$$\begin{aligned}\vec{D}_\alpha &= \left|\vec{C}_1 \cdot \vec{X}_\alpha - \vec{X}\right|, \vec{D}_\beta = \left|\vec{C}_2 \cdot \vec{X}_\beta - \vec{X}\right|, \vec{D}_\delta \\ &= \left|\vec{C}_3 \cdot \vec{X}_\delta - \vec{X}\right|\end{aligned} \tag{5}$$

$$\begin{aligned}\vec{X}_1 &= \vec{X}_\alpha - \vec{A}_1 \cdot \left(\vec{D}_\alpha\right), \vec{X}_2 = \vec{X}_\beta - \vec{A}_2 \cdot \left(\vec{D}_\beta\right), \vec{X}_3 \\ &= \vec{X}_\delta - \vec{A}_3 \cdot \left(\vec{D}_\delta\right)\end{aligned} \tag{6}$$

$$\vec{X}(t+1) = \frac{\vec{X}_1 + \vec{X}_2 + \vec{X}_3}{3} \tag{7}$$

Figure 5 illustrates how an omega updates its position with respect to the positions of alpha, beta, and delta, in a 2D search space. It can easily be deduced that the final position of an omega would be at a random place within a circle defined by the positions of alpha, beta, and delta, i.e., the omegas update their positions randomly around the prey.[17]

Attacking prey (exploitation)

Grey wolves finish the hunting process by attacking their prey. In order to mathematically model the approaching of wolves towards the prey, the value of the vector $\vec{a}$ is linearly decreased from 2 to 0 over the entire iteration. So, the fluctuation range of $\vec{A}$ is also decreased by $\vec{a}$, i.e., $\vec{A}$ can be any arbitrary value in

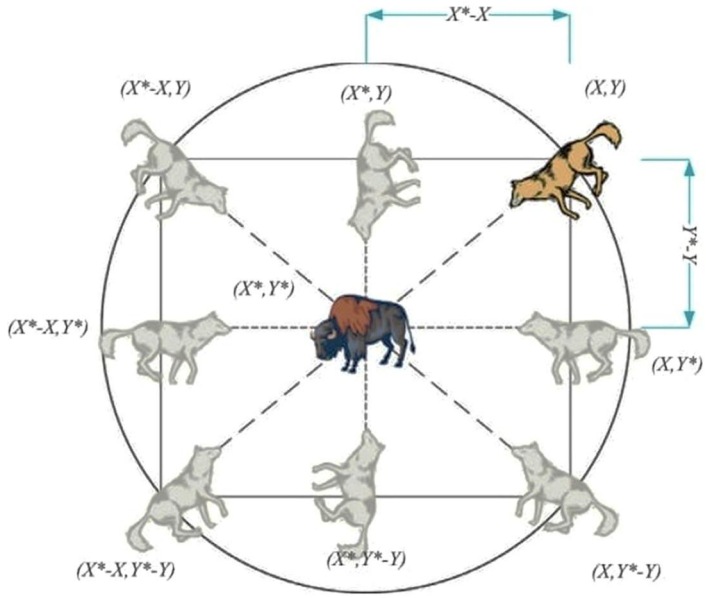

Figure 3. Possible positions in a 2D space.[17]

the interval $[-a,a]$. When the random values of $\vec{A}$ are in the interval $[-1,1]$, the location of the search agent can be anywhere between its current position and the location of prey. Hence,when $|A| < 1$, the wolves tend to attack their prey, as illustrated in Fig. 6.

Search for prey (exploration)

Grey wolves hunt mostly according to the positions of alpha, beta, and delta. They converge to attack a prey and diverge to search for a (better) prey. Random values of $\vec{A}$ which are greater than 1 and less than −1, i.e., $|A| > 1$are utilized, in order to model this diverging behavior of grey wolves. This forces the wolves to diverge from a prey and search for a (better) prey, as shown in Fig. 7. Another factor that helps in the exploration process is a random vector C, which has random values in the interval [0,2]. This vector assigns importance to a prey, i.e., to emphasize $(C > 1)$ or de-emphasize $(C < 1)$ the effect of prey in defining the distance in Eq. (1). This helps in providing a more random behavior throughout the optimization process, favoring local optima avoidance as well as exploration. It is worthwhile to mention here that unlike a, the values of C are not decreased linearly over the course, instead, random values are chosen deliberately for exploration not only in the initial stages but throughout the entire run. Different positions around the alpha wolf can be reached while varying the values of vectors A and C. From the formulation, it can be observed that vector A lies between $-a$ to $+a$, since the random variable r_1 as well as r_2 is in the interval [0,1]. As a is decreased from 2 to 0, A lies between [−2,2]. So, when the value of A is between [−1,1], it enacts attacking the prey, whereas, in the remaining cases, it enacts leaving the prey in

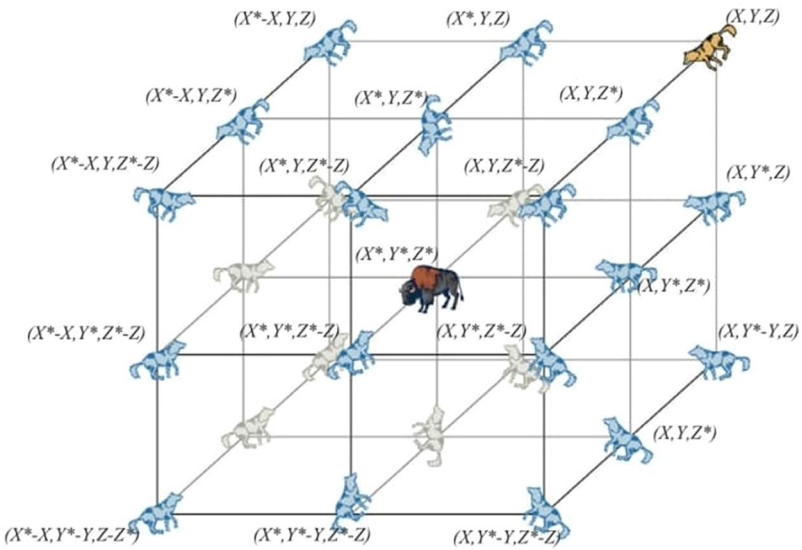

Figure 4. Possible positions in a 3D hypercube.[17]

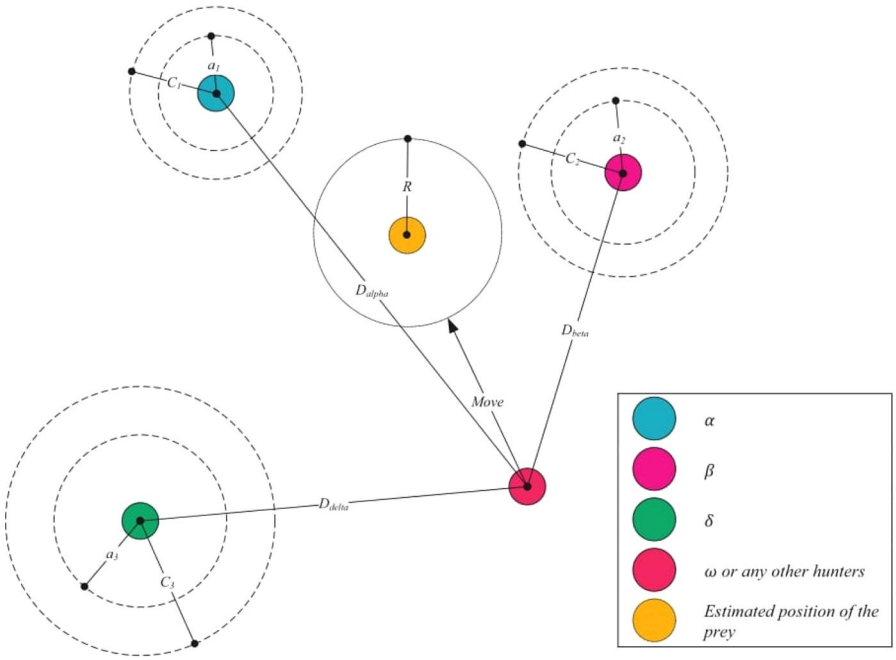

Figure 5. Position updating in GWO. *Note*: GWO, grey wolf optimizer.[17]

order to search for a better prey. As for the values of C, it lies between 0 and 2 and is random in nature. From Eq. (1), it can be observed that different weights are assigned to the distances of the wolf from prey, either emphasizing or de-emphasizing the ability of a wolf to approach a prey.

The pseudo code of GWO is presented as below:

1. Initialize the grey wolf population X_i $(i = 1, 2,\ldots,n)$
2. Initialize a, A, and C
3. Calculate the fitness of each search agent in the search space
4. $X_\alpha =$ the best search agent
5. $X_\beta =$ the second best search agent
6. $X_\delta =$ the third best search agent
7. while ($t <$ maximum number of iterations)
8. for each search agent
9. Update the position of the current search agent by Eq. (7)
10. end for
11. Update a, A, and C
12. Calculate the fitness of all search agents
13. Update X_α, X_β, and X_δ
14. $t = t + 1$
15. end while
16. return X_α

The GWO has several predominant advantages over the other population-based optimization algorithms, as mentioned here-in-under.

a. The concept of social hierarchy helps GWO to save the best solutions after every iteration.
b. The search space around the prey can be extended to multiple dimensions, as required by the optimization problem.
c. The random parameters C and A help the prospective solutions in hunting and searching for prey by encircling around them.

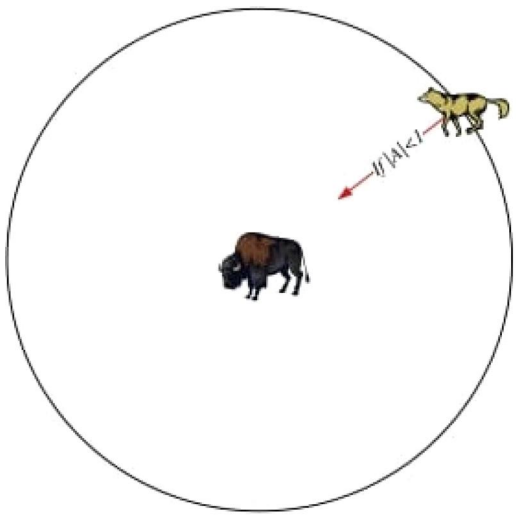

Figure 6. Exploitation (hunting).[17]

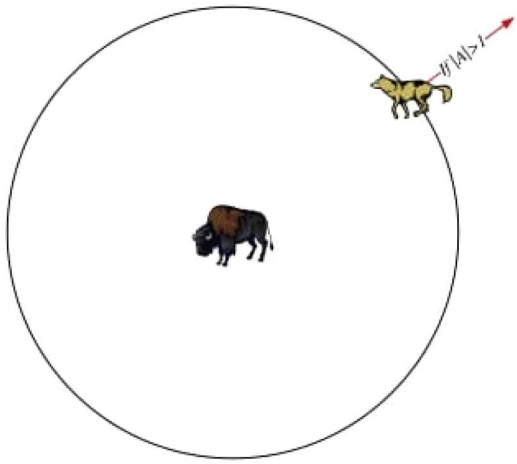

Figure 7. Exploration (searching).[17]

d. With decreasing values of A, half of the iterations are dedicated to exploitation ($|A| < 1$) and the other half is dedicated to exploration ($|A| > 1$).
e. It has only two adjustable parameters, i.e., a and C.

This algorithm is now applied for parametric optimization of two AWJM processes and the derived optimal solutions are compared with those already attained by the other population-based algorithms. The flow chart of GWO is exhibited in Fig. 8.

Results and Discussion

A MATLAB code is developed based on the mathematical models described in the previous sub-sections and is adopted to determine the optimal parametric settings of two AWJM processes. The corresponding source code of GWO is subsequently run on MATLAB R2011a, 4.00 GB RAM, 32-bit OS and 2.30 GHz processor operating platform. In the first example, based on an empirical model developed by Hashish,[1] an attempt is made to maximize MRR with respect to several defined constraints. In the second example, two AWJM responses, i.e., MRR and SR are simultaneously optimized with respect to the constrained values of some of the process parameters. In this example, for multi-objective optimization of the responses, the developed Pareto front will provide a non-dominated set of solutions. The scatter diagrams will also help in investigating the influences of the considered AWJM process parameters on the responses and guiding the process engineers in setting the optimal parametric combinations for achieving enhanced machining performance.

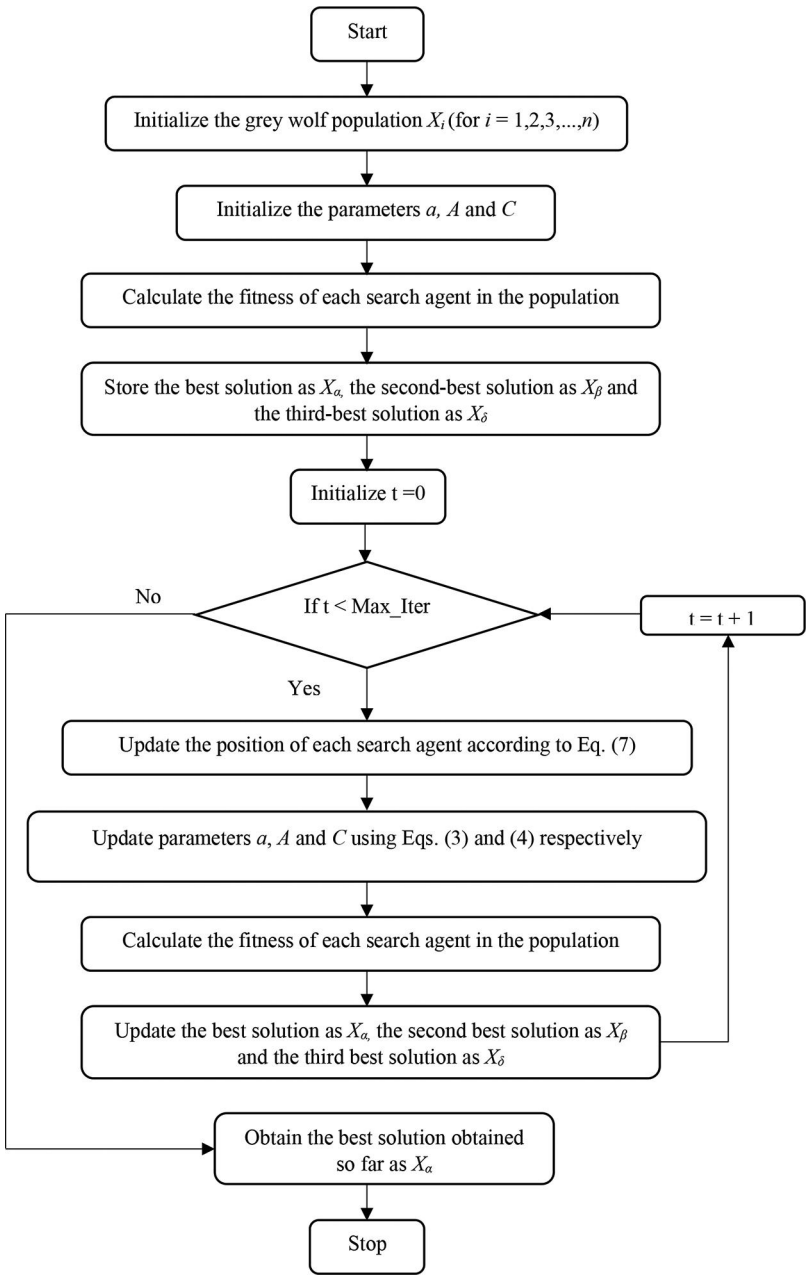

Figure 8. Flowchart of GWO. *Note*: GWO, grey wolf optimizer.

Example 1

It was already mentioned that AWJM is a hybrid NTM process combining the material removal mechanisms of both AJM and WJM processes as it uses a high velocity jet of abrasive particles mixed with water as the cutting tool. A stream of fine abrasive particles is propelled by a high velocity waterjet, which gives the mixture a high momentum when it strikes the workpiece surface. The important control parameters of an AWJM process can be classified as hydraulic parameters: water pressure and water flow rate; abrasive parameters: type, size, shape and flow rate of abrasive particles; and cutting parameters: traverse rate and stand-off-distance. Pawar and Rao[7] considered the mathematical model as developed by Hashish,[1] depicting the interrelationship between MRR and five control parameters of an AWJM process. The decision variables (control parameters), objective function and constraints considered in that model are given as below:

Decision variables: Diameter of abrasive water-jet nozzle (d_{awn}) (in mm), feed rate of nozzle (f_n) (in (mm/s), mass flow rate of abrasives (M_a) (in kg/s), water-jet pressure at nozzle exit (P_w) (in MPa), and mass flow rate of water (M_w) (in kg/s)

Objective function: Maximize MRR (Z)

$$Z = d_{awn}\, f_n (h_c + h_d) \tag{8}$$

where h_c is the indentation depth due to cutting wear, as given by Eqs. (9) and (10).

$$h_c = \left(\frac{1.028 \times 10^{4.5}\xi}{C_k \rho_a^{0.4}}\right)\left(\frac{d_{awn}^{0.2} M_a^{0.4}}{f_n^{0.4}}\right)\left(\frac{M_w P_w^{0.5}}{M_a + M_w}\right) - \left(\frac{18.48 K_a^{2/3}\xi^{1/3}}{C_k^{1/3} f_r^{0.4}}\right)\left(\frac{M_w P_w^{0.5}}{M_a + M_w}\right)^{1/3}; \text{if } \alpha_t \le \alpha_0 \tag{9}$$

$$h_c = 0, \text{ if } \alpha_t \ge \alpha_0 \tag{10}$$

Table 1. Values of constants and parameters in Example 1.

Notation	Description	Unit	Value
ρ_a	Density of abrasive particles	kg/mm^3	3.95×10^{-6}
v_a	Poisson ratio of abrasive particles		0.25
E_{Ya}	Modulus of elasticity of abrasive particles	MPa	350,000
f_r	Roundness factor of abrasive particles		0.35
f_s	Sphericity factor of abrasive particles		0.78
η_a	Proportion of abrasive grains effectively participating in machining		0.07
v_w	Poisson ratio of work material		0.20
E_{Yw}	Modulus of elasticity of work material	MPa	114,000
σ_{ew}	Elastic limit of work material	MPa	883
σ_{fw}	Flow stress of work material	MPa	8,142
C_{fw}	Drag friction coefficient of work material		0.002
ξ	Mixing efficiency between abrasive and water		0.8
P_{max}	Allowable power consumption value	kW	56

h_d is the indentation depth due to deformation wear, as given in Eq. (11).

$$h_d = \frac{\eta_a d_{awn} M_a [K_1 M_w P_w^{0.5} - (M_a + M_w) v_{ac}]^2}{(1570.8\sigma_{fw}) d_{awn}^2 f_n (M_a + M_w)^2 + (K_1 C_{fw} \eta_a)[K_1 M_w P_w^{0.5} - (M_a + M_w) v_{ac}] M_a M_w P_w^{0.5}} \tag{11}$$

$$\alpha_0 \approx \left(\frac{0.02164 C_k^{1/3} f_r^{0.4}}{K_a^{2/3}\xi^{1/3}}\right)\left(\frac{M_a + M_w}{M_w P_w^{0.5}}\right)^{1/3} \text{(degrees)} \tag{12}$$

$$\alpha_t \approx \left(\frac{0.389 \times 10^{-4.5} \rho_a^{0.4} C_k}{\xi}\right)\left(\frac{d_{awn}^{0.8} f_n^{0.4} (M_a + M_w)}{M_a^{0.4} M_w P_w^{0.5}}\right) \text{(degrees)} \tag{13}$$

$$v_{ac} = 5\pi^2 \frac{\sigma_{ew}^{2.5}}{\rho_a^{0.5}}\left[\frac{1 - v_a^2}{E_{Ya}} + \frac{1 - v_w^2}{E_{Yw}}\right]^2 \text{(mm/s)} \tag{14}$$

$$K_1 = \sqrt{2} \times 10^{4.5}\xi \tag{15}$$

$$C_k = \sqrt{\frac{3000\sigma_{fw} f_r^{0.6}}{\rho_a}} \text{(mm/s)} \tag{16}$$

$$K_a = 3 \tag{17}$$

Constraint

Constraint is on power consumption, which is given by Eq. (18).

$$1.0 - \frac{P_w M_w}{P_{max}} \ge 0 \tag{18}$$

Descriptions of various symbols appearing in Eqs. (8) to (18) are given in Table 1.

Variable bounds

The bounds for the five considered variables are given in Eqs. (19)–(23).

$$50 \le P_w \le 400 \tag{19}$$

$$0.5 \le d_{awn} \le 5 \tag{20}$$

$$0.2 \le f_n \le 25 \tag{21}$$

$$0.02 \le M_w \le 0.2 \tag{22}$$

$$0.0003 \le M_a \le 0.08 \tag{23}$$

These lower and upper bounds of the control parameters act as constraints to the optimization problem. Considering values for parameters spanning the whole real domain is infeasible in terms of technology as well as process capability. In order to model the process, a fixed range for parameters is required for conducting a finite number of experiments, while keeping in mind the technology as well as process constraints.

Hashish[1] adopted GA technique in order to find out the maximum value of MRR as 90.257 mm^3/s and observed the following settings for abrasive water-jet nozzle diameter, feed

Table 2. Single objective optimization results for Example 1.

Method	d_{awn}	f_n	M_w	P_w	M_a	α_0	α_1	h_c	h_d	MRR	Power
GA[1]	3.726	23.17	0.141	398.3	0.079	0.384	0.572	0	1.045	90.257	56
SA[19]	2.9	15	0.138	400	0.08	0.385	0.378	2.97	2.04	218.19	56
TLBO[7]	5.0	5.404	0.141	400	0.07	0.379	0.350	5.694	3.238	239.54	56
GWO	5.0	10.43	0.139	399.9	0.079	0.3847	0.3845	4.1604	1.7387	307.639	56

GA, genetic algorithm; GWO, grey wolf optimizer; MRR, material removal rate; SA, simulated annealing; TLBO, teaching-learning-based optimization.

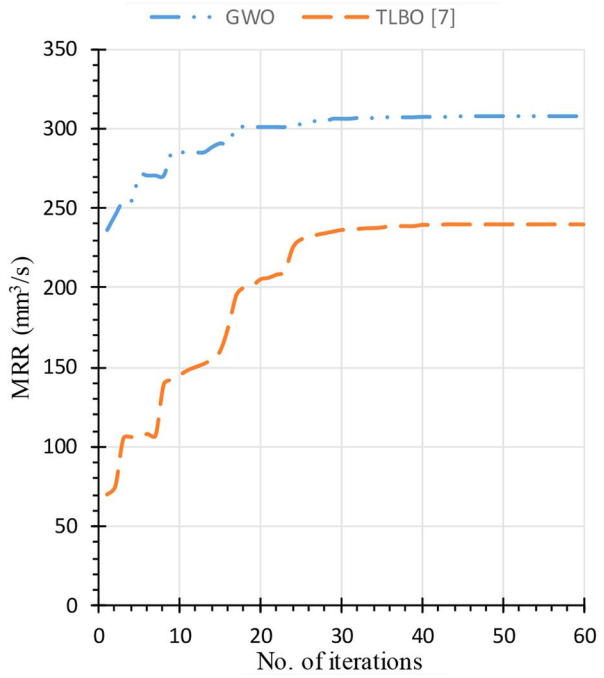

Figure 9. Convergence diagram of GWO as compared to TLBO algorithm. *Note*: GWO, grey wolf optimizer; MRR, material removal rate; TLBO, teaching-learning-based optimization.

rate of nozzle, mass flow rate of water, water-jet pressure at nozzle exit, mass flow rate of abrasives as 3.726 mm, 23.17 mm/s, 0.141 kg/s, 398.3 MPa, and 0.079 kg/s respectively. On the other hand, Paul et al.[19] applied SA technique for solving the same constrained single-objective optimization problem and derived the settings for the considered process parameters as 2.9 mm, 15 mm/s, 0.138 kg/s, 400 MPa, and 0.08 kg/s respectively, with an improvement in MRR value, from 90.257 to 218.19 mm^3/s. The application of TLBO algorithm[7] observed a further increment in MRR value to 239.54 mm^3/s, with an optimal parametric setting as 5 mm, 5.404 mm/s, 0.141 kg/s, 400 MPa, and 0.07 kg/s. In this paper, GWO is employed to determine the optimal combinations of AWJM process parameters in an attempt to achieve a higher MRR value. The derived results are presented in Table 2, along with the comparison of the optimal solutions with those as attained by the other algorithms. It shows that for GWO, there is a remarkable improvement in MRR value. Figure 9 shows the convergence diagram of both GWO and TLBO[7] algorithms and it is clearly observed that GWO converges quite fast towards the optimal MRR value.

In Fig. 10, scatter plots are generated in order to show the variations in MRR with varying values of different AWJM process parameters. These plots provide a better insight into

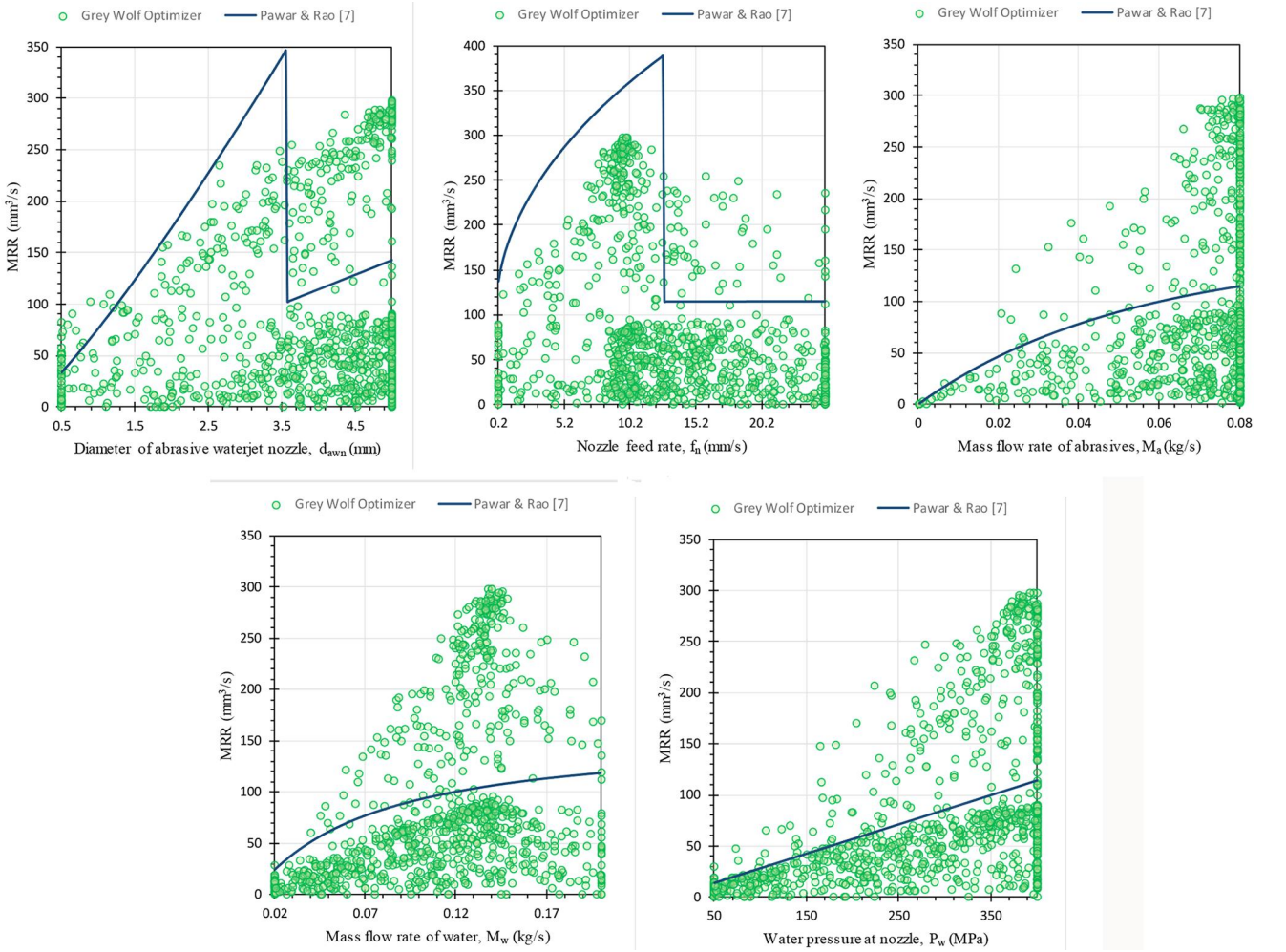

Figure 10. Variations in MRR with different AWJM process parameters. *Note*: AWJM, abrasive water-jet machining; MRR, material removal rate.

Table 3. Different process parameters in Example 2.

Parameter	Symbol	Coded levels. −1	0	+1
Water pressure (P) (MPa)	x_1	190	250	310
Jet feed speed (u) (mm/s)	x_2	0.05	0.15	0.25
Abrasive mass flow rate (m_a) (g/s)	x_3	3.5	7.5	11.5
Surface speed (V_s) (m/s)	x_4	1.5	5.5	9.5
Nozzle tilted angle (β) (°)	x_5	45	75	105

how an output response behaves with variations in several process parameters, as opposed to surface plots, where only variation of a response with respect to a particular process parameter is portrayed whilst other parameters are kept constant. From these scatter plots, it can be observed that there is a sharp edge in the trend of MRR with variations in diameter of abrasive water-jet nozzle and nozzle feed rate, as already investigated by Hashish.[1] In AWJM process, if the angle of impingement at the top of the surface (α_t) exceeds the critical impact angle (α_o), it is then assumed that there is no material removal due to cutting wear, and material removal only occurs due to deformation wear. The angle of impingement is a dependant variable (not a process parameter) as its value changes over the course of iterations with the varying values of other parameters. Hence, a sudden drop in MRR is observed in Fig. 10, as the angle of impingement exceeds the critical impact angle. These plots thus show a range of values for the considered process parameters, where MRR is the maximum, just before the critical impact angle (i.e., the moment after which MRR drastically drops). From the results obtained by GWO in Table 2, it can be observed that the angle of impingement is just less than the critical impact angle, when the maximum MRR is attained. From Fig. 10, it can also be observed that MRR increases with the increase in the values of mass flow rate of the abrasives, water pressure at nozzle and mass flow rate of water. These scatter plots will be of immense help to the process engineers and operators for choosing the best parametric mix so as to achieve maximum MRR value.

Table 4. A complete set of non-dominated solutions.

MRR (μm³/μs)	SR (μm)	P (MPa)	u (mm/s)	m_a (g/s)	V_s (m/s)	β (°)
6769.597	4.10484	310	0.05	11.5	7.267935	115
6764.853	4.099072	310	0.05	11.5	7.279354	114.2059
6760.95	4.094221	310	0.05	11.5	7.253721	113.553
6754.199	4.087944	310	0.05	11.5	7.42053	112.5231
6681.881	4.01909	310	0.05	11.5	6.559457	102.5815
6648.86	3.988563	310	0.05	11.5	6.810854	95.7276
6352.671	3.885571	299.5145	0.05	11.5	7.181496	92.64644
5899.308	3.740344	286.5486	0.05	10.71676	6.648161	80.29241
5144.083	3.481679	256.5656	0.05	11.5	5.93455	94.47595
4253.454	3.081091	216.3119	0.05	11.5	6.560403	61.25093
3766.111	2.847155	190	0.05	10.72347	6.149893	58.74609
3701.705	2.84601	190.789	0.05	10.59956	6.116283	70.46296
3687.107	2.835886	190	0.05	10.7109	6.117306	68.30723
3532.209	2.786867	190	0.05	10.98489	4.051548	54.70002
3404.177	2.780198	191.126	0.05	11.5	3.881486	57.28654
3397.165	2.773943	190	0.05	11.5	3.803904	53.30112
3274.123	2.748508	190	0.05	10.63846	2.601239	58.0797
3268.064	2.747387	190	0.05	10.74025	2.66389	58.33875
3228.336	2.74207	190	0.05	10.97474	2.568462	54.82565
3185.448	2.740137	190	0.05	10.46431	2.133598	58.45391
3114.819	2.730917	190	0.05	11.04623	2.041321	50.17717
2984.425	2.715399	190	0.05	10.72999	1.5	55.15272
2925.517	2.709523	190	0.05	10.93446	1.5	57.09611
2891.393	2.706028	190	0.05	11.16296	1.5	55.07382
2867.242	2.705975	190	0.05	11.30765	1.619419	58.29498
2839.107	2.702729	190	0.05	11.38135	1.5	55.16243
2809.658	2.701205	190	0.05	11.47643	1.5	55.90055
2804.542	2.701011	190	0.05	11.5	1.5	55.8091
2800.53	2.700773	190	0.05	11.5	1.5	56.29404
2797.571	2.700624	190	0.05	11.5	1.5	56.65165
2794.179	2.70048	190	0.05	11.5	1.5	57.06175
2791.079	2.700375	190	0.05	11.5	1.5	57.43642
2787.672	2.700287	190	0.05	11.5	1.5	57.8483
2785.61	2.700249	190	0.05	11.5	1.5	58.09755

MRR, material removal rate; SR, surface roughness.

Example 2

Yue et al.[20] performed an experimental investigation on a radial mode abrasive water-jet turning operation of 96% alumina ceramic to explore the influences of various AWJM process parameters (i.e., water pressure, jet feed speed, abrasive mass flow rate, surface speed and nozzle tilted angle) on MRR and SR. Table 3 exhibits different process parameters and their levels as set for the said machining operation. Based on the experimental data and using RSM technique, the following two non-linear regression models were developed which are subsequently employed for multi-objective optimization of AWJM responses and development of the related optimal Pareto front.

$$\begin{aligned} \mathrm{MRR} = {} & 3814.35 + 943.5x_1 - 530.28x_2 + 745.01x_3 \\ & + 154.83x_4 - 193.65x_5 + 551.62x_1x_3 + 284.87x_1x_5 \\ & - 147.61x_2x_5 + 225.72x_3x_4 + 345.29x_2^2 - 430.00x_4^2 \end{aligned} \tag{24}$$

$$\begin{aligned} R_a = {} & 3.78 + 0.31x_1 + 0.04x_2 - 0.38x_3 + 0.087x_4 \\ & + 0.046x_5 - 0.24x_1x_2 - 0.067x_4x_5 - 0.17x_2^2 \\ & + 0.17x_3^2 + 0.14x_5^2 \end{aligned} \tag{25}$$

Yue et al.[20] applied sequential approximation optimization technique to optimize both MRR and SR, i.e., maximize MRR and minimize SR simultaneously. The optimal parametric settings were derived as water pressure = 310 MPa, jet feed speed = 0.25 mm/s, abrasive mass flow rate = 11.5 g/s, surface speed = 6 m/s, and nozzle tilted angle = 71°. At these optimal settings, the MRR and SR were obtained as 5441.96 μm³/μs and 3.41 μm respectively. However, in this type of multi-objective optimization problem, weight (relative importance) assigned to each of the responses plays an important role. Allocation of different weights to different responses may often lead to changing values of the optimal parametric settings. The technique adopted by Yue et al.[20] did not provide any guidance for choosing the weights of the responses. For this example, an optimal Pareto front is thus generated so as to provide a set of non-dominated solutions, which may guide the process engineers in determining different combinations of weights for the responses, and these solutions being non-dominated, make each solution as the best one.

In this example consisting of simultaneous optimization of both MRR and SR, using GWO, MRR is maximized at the first run, and the sets of all the points generated throughout the iterations are collected. These sets of points (parametric settings) show a convergence towards the maximum possible

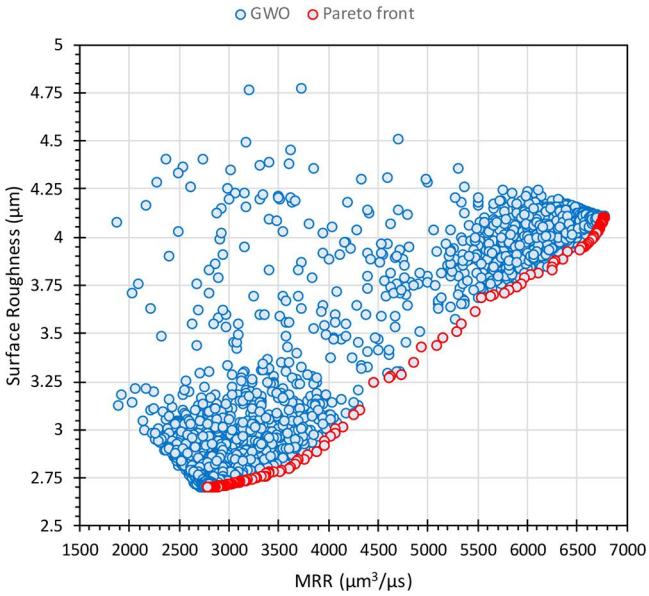

Figure 11. A complete set of Pareto points. *Note*: GWO, grey wolf optimizer; MRR, material removal rate.

MRR. During the second run, SR response is again separately minimized using the same algorithm to obtain similar sets of points. These points show a trend towards the minimum achievable SR value. These two datasets are then combined together and an optimal Pareto front is thus generated for MRR versus SR, i.e., a set of non-dominated solutions is developed, which simultaneously has the best (maximum) MRR and the best (minimum) SR. A set of 34 such solution sets is provided in Table 4 and the full set of the Pareto optimal solutions is plotted in Fig. 11. Two extreme solutions are shown below:

a. For highest MRR of 6769.597 $\mu m^3/\mu s$ and highest SR of 4.10484 μm, the parametric settings are water pressure = 310 MPa, jet feed speed = 0.05 mm/s, abrasive mass flow rate = 11.5 g/s, surface speed = 7.267935 m/s, and nozzle tilted angle = 115°.
b. For least MRR of 2785.61 $\mu m^3/\mu s$ and least SR of 2.700249 μm, the parametric combinations are water pressure = 190 MPa, jet feed speed = 0.05 mm/s, abrasive mass flow rate = 11.5 g/s, surface speed = 1.5 m/s, and nozzle tilted angle = 58.09755°.

The intermediate settings also provide a compromise between the two responses, which will serve as a guide to the process engineers and operators for selecting the optimal parametric settings. In order to study variations of MRR and SR with changing values of different AWJM process parameters, scatter plots are also developed, and the trends obtained using GWO are compared with those predicted by Yue et al.[20].

From Fig. 12(a), it can be observed that MRR increases with water pressure. As the water pressure increases, there is a

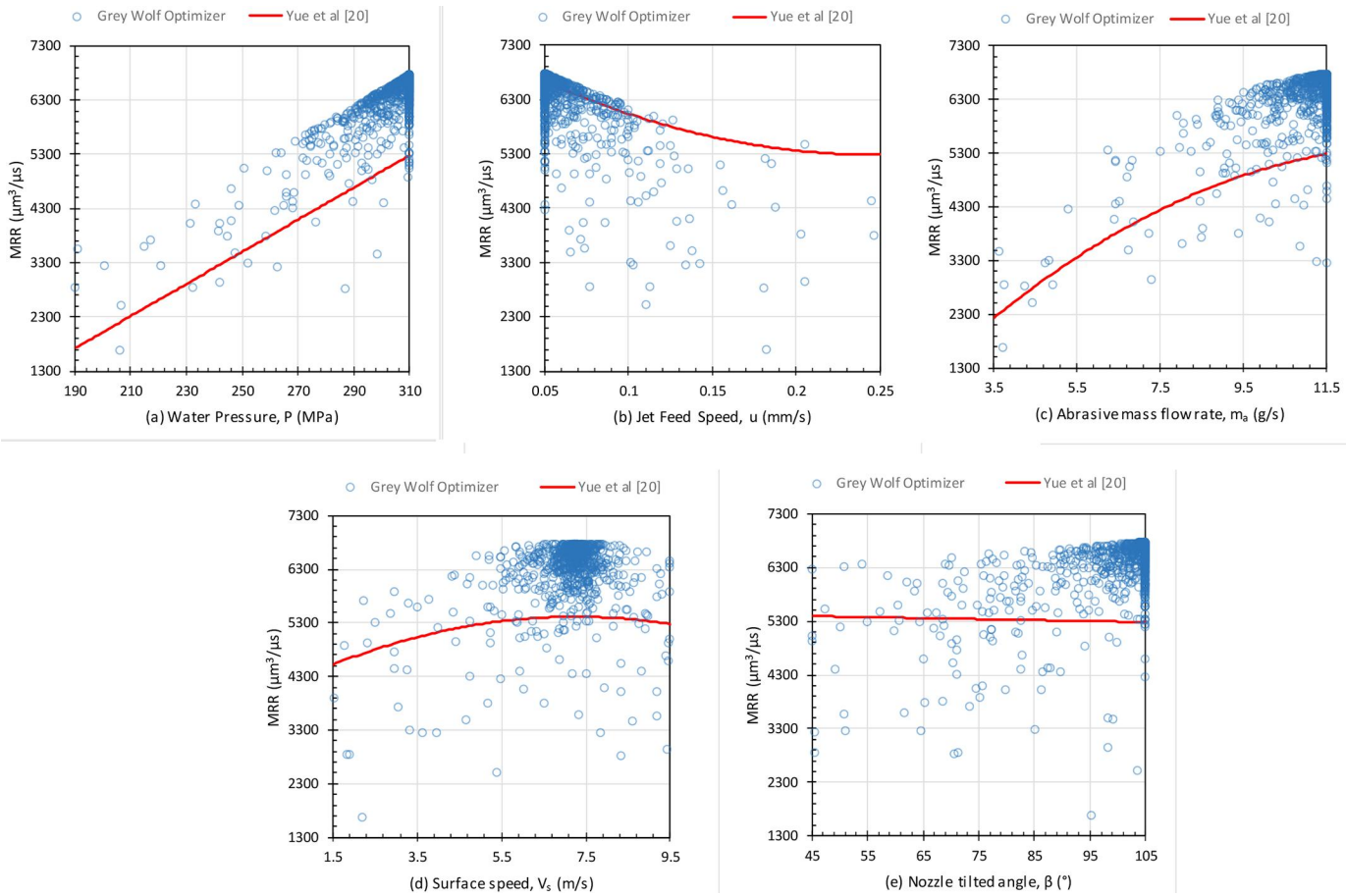

Figure 12. Variations in MRR with AWJM process parameters for Example 2. *Note*: AWJM, abrasive water-jet machining; MRR, material removal rate.

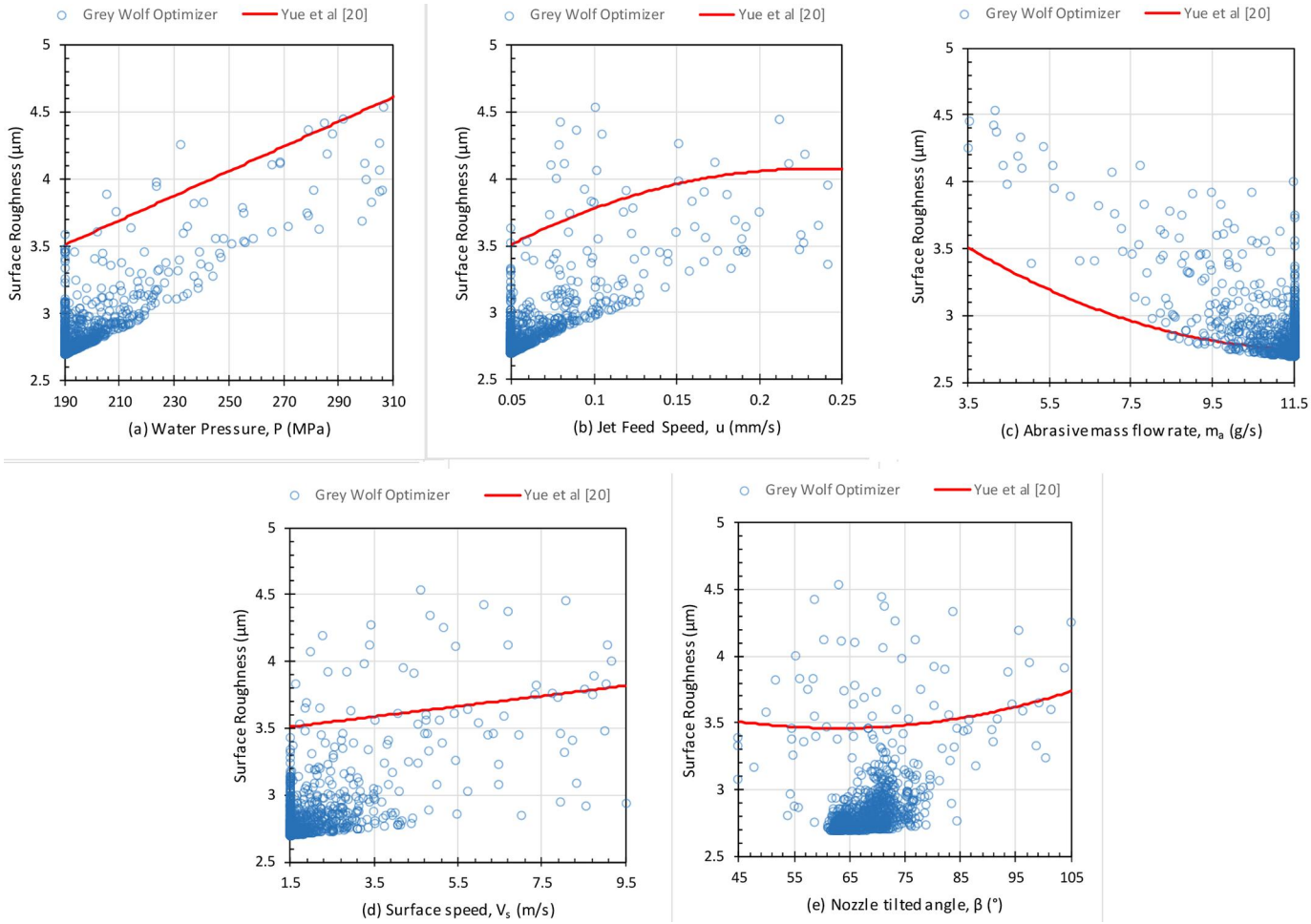

Figure 13. Variations in SR with AWM process parameters for Example 2. *Note*: AWJM, abrasive water-jet machining; SR, surface roughness.

certain increase in the velocity of the abrasive particles striking the workpiece surface, which in turn, implies that abrasive particles with higher kinetic energy imparted on the surface resulting in an increase in depth of cut as well as MRR. However, MRR decreases with increase in jet feed speed, as shown in Fig. 12(b). As the velocity distribution is not clearly known, it has been assumed by the past researchers[21] to follow a Gaussian distribution, with the velocity of particles in the core being maximum and bare minimum at the boundary. So, the particles in the core having higher kinetic energy participate in the maximum amount of material removal, along with the boundary particles enhancing the erosion. As the jet feed speed decreases, the exposed time of the jet to the surface increases, which in turn, results in more material removal and more penetration. In Fig. 12(c), MRR is also observed to have an increasing trend with respect to abrasive mass flow rate. However, at higher flow rates, the cutting efficiency decreases due to increase in the abrasive interactions. For surface speed, it can be observed from Fig. 12(d) that the optimal surface speed can be maintained around 6.5 ~ 8 m/s.

The MRR also increases as the nozzle tilted angle increases, as observed in Fig. 12(e). For SR response, it can be observed from Fig. 13(a), 13(b), and 13(d) that it reaches its minimum at lower values of water pressure, jet feed speed and surface feed. However, an increase in abrasive mass flow rate helps in producing a better surface finish, as shown in Fig. 13(c). For nozzle tilted angle, a value around 50° ~ 70° can be set for attaining thebest surface finish, as indicated in Fig. 13(e).

Conclusion

In this paper, an attempt is made for parametric optimization of two AWJM processes using an almost unexplored optimization tool in the form of GWO. The results derived from both the single objective and multi-objective optimization problems are observed to be quite satisfactory when compared to other algorithms, such as SA, GA, and TLBO. The developed convergence diagram shows a high convergence rate of this algorithm towards the optimal solution, owing to the effects of its different control parameters (a and C), which maintain a good balance between exploration and exploitation. This algorithm is also proved to be faster in tracking down the prey (finding out the optimal solution), because of the presence of a social hierarchy of grey wolves. The developed scatter diagrams, exhibiting the variations of different responses with respect to the changing values of various AWJM process parameters would be of great help to the process engineers and operators in setting those parameters as their optimal levels so as to achieve maximum machining performance. As an

empirical formulation and results derived by the past researchers are utilized in this paper, there is no scope for any confirmatory experiment so as to validate the solutions. In future, this algorithm can also be adopted for parametric optimization of other advanced manufacturing processes.

References

[1] Hashish, M. A Model for Abrasive Water Jet (AWJ) Machining. *J. Eng. Mater. Technol.* **1989**, *111*, 154–162. DOI: 10.1115/1.3226448.

[2] Jain, N. K.; Jain, V. K.; Deb, K. Optimization of Process Parameters of Mechanical Type Advanced Machining Processes Using Genetic Algorithms. *Int. J. Mach. Tools Manuf.* **2007**, *47*, 900–919. DOI: 10.1016/j.ijmachtools.2006.08.001.

[3] Çaydaş, U.; Hasçalık, A. A Study on Surface Roughness in Abrasive Waterjet Machining Process Using Artificial Neural Networks and Regression Analysis Method. *J. Mater. Process. Technol.* **2008**, *202*, 574–582. DOI: 10.1016/j.jmatprotec.2007.10.024.

[4] Zain, A. M.; Haron, H.; Sharif, S. Optimization of Process Parameters in the Abrasive Waterjet Machining Using Integrated SA-GA. *Appl. Soft Comput.* **2011**, *11*, 5350–5359. DOI: 10.1016/j.asoc.2011.05.024.

[5] Zain, A. M.; Haron, H.; Sharif, S. Estimation of the Minimum Machining Performance in the Abrasive Waterjet Machining Using Integrated ANN-SA. *Expert Syst. Appl.* **2011**, *38*, 8316–8326. DOI: 10.1016/j.eswa.2011.01.019.

[6] Aultrin, K. S. J.; Anand, M. D.; Jose, P. J. Modelling the Cutting Process and Cutting Performance in Abrasive Waterjet Machining Using Genetic-Fuzzy Approach. *Procedia Eng.* **2012**, *38*, 4013–4020. DOI: 10.1016/j.proeng.2012.06.459.

[7] Pawar, P. J.; Rao, R. V. Parameter Optimization of Machining Processes Using Teaching-Learning-Based Optimization Algorithm. *Int. J. Adv. Manuf. Technol.* **2013**, *67*, 995–1006. DOI: 10.1007/s00170-013-4961-6.

[8] Yusup, N.; Sarkheyli, A.; Zain, A. M.; Hashim, S.Z. M.; Ithnin, N. Estimation of Optimal Machining Control Parameters Using Artificial Bee Colony. *J. Intell. Manuf.* **2014**, *25*, 1463–1472. DOI: 10.1007/s10845-013-0753-y.

[9] Mohamad, A.; Zain, A. M.; Bazin, N.E. N.; Udin, A. A Process Prediction Model Based on Cuckoo Algorithm for Abrasive Waterjet Machining. *J. Intell. Manuf.* **2015**, *26*, 1247–1252. DOI: 10.1007/s10845-013-0853-8.

[10] Aultrin, K. S. J.; Anand, M. D. Multi-Objective Optimization of Abrasive Water Jet Machining of Aluminium 6061 Alloy by Grey Relational Analysis. *J. Chem. Pharm. Sci.* **2016**, *9*, 410–417.

[11] Jagadish; Bhowmik, S.; Ray, A. Prediction and Optimization of Process Parameters of Green Composites in AWJM Process Using Response Surface Methodology. *Int. J. Adv. Manuf. Technol.* **2016**, *87*, 1359–1370. DOI: 10.1007/s00170-015-8281-x.

[12] Kubade, P. R.; Patil, P.; Bidgar, A.; Papti, A.; Potdar, P.; Kshirsagar, R. G. Parametric Optimization of Abrasive Water Jet Machining of Inconel-718 Material. *Int. Res. J. Eng. Technol.* **2016**, *3*, 1236–1242.

[13] Lohar, S. R.; Kubade, P. R. Investigation of Effect of Abrasive Water Jet Machining (AWJM) Process Parameters on Performance Characteristics of High Carbon High Chromium Steel (AISI D3). *Int. Adv. Res. J. Sci. Eng. Technol.* **2017**, *4*,152–158. DOI: 10.17148/iarjset/ncdmete.2017.35.

[14] Shukla, R.; Singh, D. Selection of Parameters for Advanced Machining Processes Using Firefly Algorithm. *Eng. Sci. Technol. Int. J.* **2017**, *20*, 212–221. DOI: 10.1016/j.jestch.2016.06.001.

[15] Dhanawade, A.; Kumar, S. Experimental Study of Delamination and Kerf Geometry of Carbon Epoxy Composite Machined by Abrasive Water Jet. *J. Compos. Mater.* **2017**, *51*, 3373–3390. DOI: 10.1177/0021998316688950.

[16] Nair, A.; Kumanan, S. Multi-Performance Optimization of Abrasive Water Jet Machining of Inconel 617 using WPCA. *Mater. Manuf. Processes* **2017**, *32*, 693–699. DOI: 10.1080/10426914.2016.1244844.

[17] Mirjalili, S.; Mirjalili, S. M.; Lewis, A. Grey Wolf Optimizer. *Adv. Eng. Software* **2014**, *69*, 46–61. DOI: 10.1016/j.advengsoft.2013.12.007.

[18] Muro, C.; Escobedo, R.; Spector, L.; Coppinger, R. Wolf-Pack (*Canis lupus*) Hunting Strategies Emerge from Simple Rules in Computational Simulations. *Behav. Process.* **2011**, *88*, 192–197. DOI: 10.1016/j.beproc.2011.09.006.

[19] Paul, S.; Hoogstrate, A. M.; van Luttervelt, C. A.; Kals, H. J. J. Analytical Modeling of the Total Depth of Cut in Abrasive Water Jet Machining of Polycrystalline Brittle Materials. *J. Mater. Process. Technol.* **1998**, *73*, 206–212. DOI: 10.1016/s0924-0136(97)00230-6.

[20] Yue, Z.; Huang, C.; Zhu, H.; Wang, J.; Yao, P.; Liu, Z. Optimization of Machining Parameters in the Abrasive Waterjet Turning of Alumina Ceramic based on the Response Surface Methodology. *Int. J. Adv. Manuf. Technol.* **2014**, *71*, 2107–2114. DOI: 10.1007/s00170-014-5624-y.

[21] Westkamper, E.; Henning, A. Modeling of Wear Mechanisms at the Abrasive Waterjet Cutting Front. In Proceedings of the WJTA American Waterjet Conference, Houston, Texas, USA, 2003.